Symmetric Large-Area Metal-Molecular Monolayer-Metal Junctions by Wedging Transfer

ARTICLE *in* ADVANCED FUNCTIONAL MATERIALS · FEBRUARY 2013

Impact Factor: 11.81 · DOI: 10.1002/adfm.201200603

4 AUTHORS, INCLUDING:

S. Krabbenborg
BASF Coatings GmbH, Muenster, Germany
19 PUBLICATIONS **143** CITATIONS
SEE PROFILE

Jurriaan Huskens
University of Twente
364 PUBLICATIONS **8,221** CITATIONS
SEE PROFILE

Wilfred G. van der Wiel
University of Twente
107 PUBLICATIONS **4,685** CITATIONS
SEE PROFILE

FULL PAPER

Symmetric Large-Area Metal-Molecular Monolayer-Metal Junctions by Wedging Transfer

Sven O. Krabbenborg, Janine G. E. Wilbers, Jurriaan Huskens, and Wilfred G. van der Wiel**

A method is described for fabricating and electrically characterizing large-area (100–400 μm²) metal-molecular monolayer-metal junctions with a relatively high overall yield of ≈45%. The measurement geometry consists of ultra-smooth (template-stripped) patterned Au bottom electrodes, combined with ultra-smooth top Au electrodes deposited using wedging transfer. The fabrication method is applied to the electrical characterization of Au-alkanethiol self-assembled monolayer-Au junctions. An exponential decay of the current density is found for increasing the chain length of the alkanethiols, in agreement with earlier studies. The symmetric device geometry, and flexibility for contacting monolayers with various end groups are important advantages compared to existing techniques for electrically characterizing molecular monolayers.

1. Introduction

Using molecular components is a promising development in modern electronics.[1–3] Studying and controlling charge transport through a single molecule or molecular monolayer are very difficult, however. Electrically contacting a molecular monolayer is easier than addressing a single molecule, and has resulted in reproducible data.[4,5] A molecular layer embedded between two contacts typically forms a tunnel barrier between them, but also gives the possibility to add electronic functionality such as rectification or conduction switching.[6–8] It is therefore useful to study these molecular layers in more detail first, before incorporating them in (single) molecular electronic devices.[5,9]

S. O. Krabbenborg, Prof. J. Huskens
Molecular Nanofabrication Group
MESA+ Institute for Nanotechnology
University of Twente
P.O. Box 217, 7500 AE Enschede,
The Netherlands
E-mail: j.huskens@utwente.nl
J. G. E. Wilbers, Prof. W. G. van der Wiel
NanoElectronics Group
MESA+ Institute for Nanotechnology
University of Twente
P.O. Box 217, 7500 AE Enschede, The Netherlands
E-mail: w.g.vanderwiel@utwente.nl

DOI: 10.1002/adfm.201200603

Although numerous techniques exist for electrically contacting molecular layers such as self-assembled monolayers (SAMs),[10] the biggest hurdle is being able to apply the top contact to create two-terminal devices in a manner that will reproducibly yield reliable junctions. Direct metal evaporation causes metal atoms to penetrate or damage the monolayer, resulting in a low yield.[11] Other methods trying to alleviate this problem, use an additional short-chain SAM,[12] have a graphene,[13] or reduced graphene oxide protective layer,[14] have an intrinsic oxide layer,[15] or introduce an extra conducting polymer layer between the monolayer and the metal top contact, which has a non-negligible resistance.[4] A low yield makes it unpractical to obtain statistically relevant numbers of measurements, while an additional layer makes it possible to generate monolayer-based tunneling junctions with high yield. However, these protective layers also introduce ambiguities in the interpretation of the electron transport data. For example, when investigating rectification in molecular junctions,[6,16] extra care needs to be taken to prove that the rectification originates from the intrinsic molecular properties.

For fabricating metal-molecular monolayer-metal junctions without a protective layer between top contact and monolayer, but also without damaging the monolayer, several techniques exist. Most are limited by the need for strong adhesion of the top contact requiring the introduction of a chemisorbing functional group at the end of the molecular adsorbate, as is the case in micro/nanotransfer printing,[17] break junctions,[18] or flip-chip lamination.[19] Only a few fabrication techniques work independently of the end group of the monolayer. Scanning tunneling microscopy (STM),[20] and conducting probe atomic force microscopy (CP-AFM) are such techniques.[21] With CP-AFM, for example, the influence of the metal work function on the tunneling current has been investigated, made possible by the independence of end group of the monolayer on the fabrication of the molecular junction.[22] A drawback, however, of these probe-based techniques is the time-consuming process of acquiring a statistically relevant number of measurements at many positions on several samples, the difficulty of exactly determining the contact area as well as that measurements with CP-AFM are influenced by the force applied, in ways that are difficult to quantify.[23,24] More importantly, these methods are incompatible with device fabrication.

To our knowledge, only one technique allows the fabrication of large-area metal-molecule-metal junctions with a relatively high yield, without posing restrictions on the end group of the monolayer.[25–27] The latest iteration of this technique, permanent modified polymer-assisted lift-off (PeMoPALO),[27] introduced electrical contacting away from the molecular junction, removed the restriction on the junction area, and introduced the possibility to make permanent contacts via wire bonding. The system was used to study Si-alkyl-Au junctions (covalently attached monolayers of alkenes with a H-passivated Si surface). However, these alkyl layers are less thoroughly studied than SAMs of, for example, *n*-alkanethiols on Au, which are extensively studied.[10,28] It is also difficult, synthetically, to vary the end group of these alkyl layers, and they are more difficult to analyze, in the sense that they incorporate not only a tunneling barrier but also a Schottky barrier.[29] A disadvantage inherent of the system is a reduced quality of the interface between the monolayer and top electrode, which affects the electrical measurements.[30]

Here, we describe a soft lithography-based method to fabricate symmetric large-area metal-molecule-metal junctions with a relatively high yield for practically obtaining statistically relevant numbers of measurements, without an additional protection layer and without the need for a chemisorbing functional group in the monolayer. It consists of template stripping,[31] to make patterned and ultra-smooth (<0.5 nm RMS) metal bottom electrodes, which is important to reduce the density of defects in the monolayer leading to shorts.[10] This is combined with a soft deposition method of ultra-smooth top electrodes embedded in cellulose acetate butyrate from water. This soft deposition method is adopted from the recently published "wedging transfer" method to deposit Au electrodes and graphene flakes.[32] The method is now–for the first time–applied to the fabrication of molecular Au-alkanethiol SAM-Au junctions, which is used here mainly as a reference system, and their electrical properties are compared to reported values of junctions fabricated by other methods with the main aim of showing the usability of this fabrication method. This is the first time that a floatation method is shown to work with metal/metal contacts, while previous reports only showed Si or oxidized Al as bottom contacts.

2. Results and Discussion

2.1. Fabrication of the Metal-Molecular Monolayer-Metal Junctions

Figure 1 schematically shows our method for fabricating metal-molecular monolayer-metal junctions. First (Figure 1A), Au metal bottom and top electrodes were defined directly on a Si/SiO_2 wafer by photolithography and metal lift-off. No adhesion layer was used, because the electrodes had to be removed from the wafer later on by means of template stripping. After the application of an anti-sticking layer on the Si/SiO_2, the bottom electrodes were embedded in optical adhesive (OA) and template stripped (TS) from the wafer (Figure 1B). TS consists of mechanically cleaving the Si/SiO_2–Au interface,[31] exposing the ultra-smooth metal surface. Ultra-smooth surfaces are

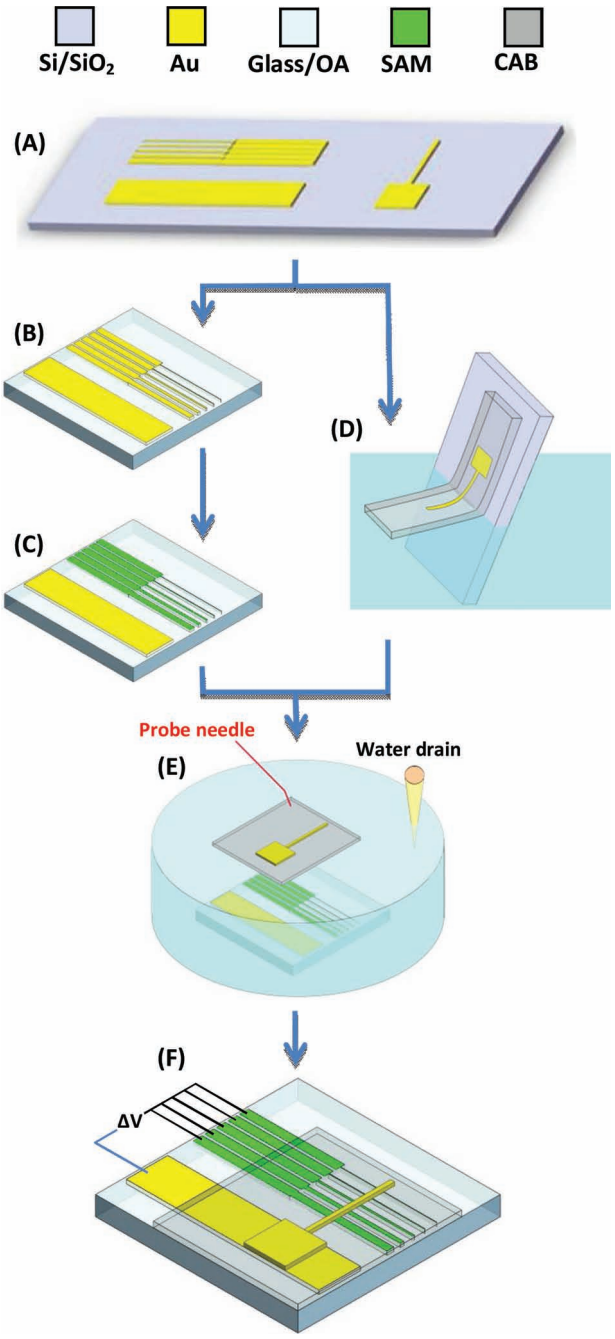

Figure 1. Scheme for the fabrication of metal-molecular monolayer-metal junctions with the wedging transfer method. A) First, Au top and bottom electrodes were fabricated on a normal Si wafer with native SiO_2. Then, after the application of an anti-sticking layer on the Si/SiO_2, a cleaned glass slide was "glued" on the bottom electrodes by means of OA, and cured by UV illumination. B) The glass slide was template stripped after curing, which caused the Au bottom electrodes to be transferred to the glass slide, with the ultra-smooth Au interface exposed, embedded in OA. C) On the ultra-smooth bottom electrodes a SAM of *n*-alkanethiol was deposited from solution, after which (D) the top electrodes were embedded in cellulose acetate butyrate (CAB) and lifted off in water. E) After aligning the top electrodes with respect to the bottom electrodes (probe needle), the molecular junctions were formed by lowering the water level (water drain). F) With the device finished, the molecular junctions were electrically characterized with probes at the blue and black positions.

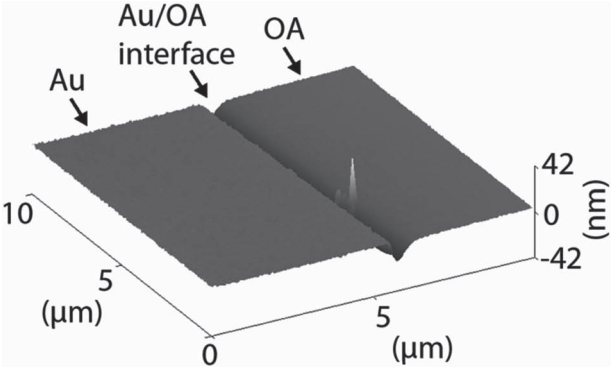

Figure 2. Tapping mode AFM height image of the Au/OA interface after TS showing the smoothness of the Au electrode and the trench next to it.

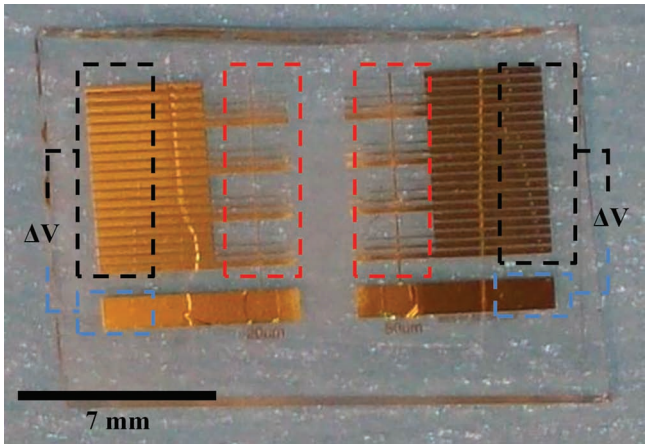

Figure 3. Photograph of the actual device, after wedging transfer, showing the molecular junctions (marked with a red box) and the electrical contacts far away from these junctions, facing upwards (probe 1 black box, probe 2 blue box).

preferred, because they lower the amount of defects in the monolayer,[10] which results in less shorts, compared to electrodes used directly after electron-beam evaporation.[33] Atomic force microscopy (AFM) on the exposed Au electrodes embedded in OA, revealed an RMS roughness of 0.27 ± 0.04 nm (scan areas of 2 μm × 2 μm), which is in the expected range for TS metal surfaces.[31,34] Embedding the metal electrodes in OA is necessary to prevent shorts at the edges of the electrodes where the monolayer is not densely packed.[10,35]

Figure 2 shows an AFM picture of an Au/OA interface after TS. It clearly shows that the Au electrode is not perfectly embedded in the OA. A trench exists next to the Au electrode, which has a width of a few 100 nm and a depth of 16 nm or more. Such a trench was reported before when TS electrodes were used.[6] This trench probably originates from shrinkage of the OA during polymerization (a linear shrinkage of 1.5% is reported by the manufacturer). Next to a trench, on several occasions the Au electrodes were found protruding from the OA by 10–15 nm (Figure S1, Supporting Information). This, together with the trench, is the most probable reason for the imperfect yield (see below).

To solve the trench and protruding electrode problems, a procedure was tried in which the bottom electrodes were embedded in PMMA. This did decrease the trenches and protrusions considerably (see Figure S2 and Figure S3, Supporting Information) indicating that OA shrinkage was the problem. However, the PMMA itself gave other problems associated with swelling after overnight immersion in ethanol. This made it impossible to fabricate molecular junctions, and therefore bottom electrodes embedded directly in OA were used for further experiments.

On the bottom electrodes a SAM of *n*-alkanethiol was deposited from solution (Figure 1C). After this, the top electrodes were embedded in a hydrophobic polymer layer of cellulose acetate butyrate by dip coating. This layer, including the metal top electrodes, was lifted off the wafer, by slowly dipping in Milli-Q water at an angle of 70° relative to the water surface (Figure 1D). This resulted in a floating polymer layer, with the embedded electrodes facing downwards. By placing the bottom electrodes below the top electrodes at the bottom of the beaker, the top electrodes were gently applied on top of the SAM by lowering the water level with a syringe pump (Figure 1E). This ensured gentle contact and prohibited shorts. Alignment was done by a probe needle, controlled with a micromanipulator that contacts the polymer layer. To ensure the removal of possible remaining water in the junction, the device was placed in a desiccator and pumped overnight. Thereafter, the molecular junctions could be electrically characterized with probes at the blue and black positions (Figure 1F). **Figure 3** shows the actual complete device.

The method for lifting-off Au electrodes without a detachment step was adopted from Dekker et al.[32] The technique is based on the hydrophobic effect,[36,37] in this case easily explaining the lift-off by the fact that water wets hydrophilic surfaces and avoids hydrophobic ones.[38–40] We show here that it also works when depositing on top of a fragile SAM. The advantage over the PeMoPALO method is that the detachment step in HF (and the consecutive cleaning step) is obsolete. Furthermore, the lift-off and application of the top electrodes was done in water, ensuring a better quality interface.[30]

Instead of applying the top electrodes embedded in cellulose acetate butyrate, while floating on the water-air interface, it was also tried to apply TS top electrodes, embedded in OA on a polydimethylsiloxane (PDMS) stamp, by hand. The procedure is shown and explained in Figure S4 (Supporting Information). The PDMS should provide conformal and soft contact. Although this approach worked, and gave the expected tunneling characteristics while electrically characterizing the resulting *n*-alkanethiol junctions, the overall yield after optimization was only 10%, compared to ≈45% when applying the wedging transfer technique, while also having a spread in current densities of seven orders of magnitude. This rendered this approach unpractical and unreliable for electrically characterizing metal-molecular monolayer-metal junctions.

The design, shown in Figure 3, incorporates electrical contact points facing upwards and far away from the molecular junctions. This gives the possibility for integration in a sample holder. Also, remote contacting of the molecular junctions ensures that electrical measurements can be done without damaging the molecular junctions.

Table 1. Working device yields and other parameters for measurements of molecular junctions with SAMs of alkanethiols of different lengths (n_c = 12–16) fabricated with the wedging transfer method.

n_c	Total number of junctions	Shorting junctions[a)]	Open circuits[b)]	Unstable junctions[c)]	N_j[d)]	Working device yield [%]
12	32	17	1	2	240	38
14	34	14	2	1	340	50
16	22	8	3	1	200	46

[a)]A short is defined in the text as a junction which has a linear, ohmic *J*–*V* curve (typical resistance of few 100 Ω); [b)]An open circuit is defined as a junction which exhibits current values in the noise level of the measurement setup (10^{-15} A); [c)]An unstable junction is defined as not belonging to the other three categories; [d)]The total number of values of *J* used for calculations.

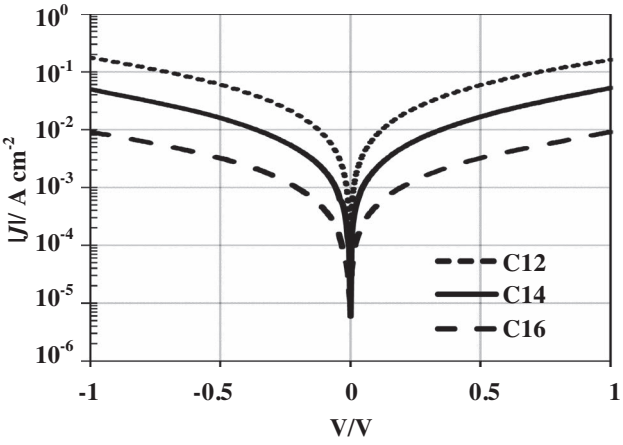

Figure 4. Plot of log-averaged |*J*| as a function of *V*, for different lengths of *n*-alkanethiols (n_c = 12–16). The plot contains a full trace (up and down), showing perfect overlap.

2.2. Electrical Characterization of the Molecular Junctions

Molecular junctions with *n*-alkanethiol SAMs (n_c = 12–16) were electrically characterized by measuring the current density, *J*, as a function of the applied voltage, *V*. For every *n*-alkanethiol a minimum of 3 separate devices were fabricated and a minimum of 22 junctions ($Au/SC_{n-1}CH_3/Au$) were measured. On each junction, 11 *J*(*V*) traces (one trace = 0 V → +1 V → –1 V → 0 V) were recorded, from which the first one was discarded. For every *n*-alkanethiol 200–340 *J*(*V*) data points were collected. All analyzed junctions had an area size between 100 and 400 μm², by changing the width of the top and/or bottom electrode by design.

Table 1 shows an overview of the total numbers of junctions measured, data points (N_j), working junction yield and other parameters, all specified per *n*-alkanethiol. A working junction is defined as a junction having a nonlinear *J*–*V* slope with currents below 10^{-3} A at 1 V applied bias (which is more than one order of magnitude higher than the highest current measured). Each junction must be measureable 11 times and these measurements should be "stable" in the sense that the current should not drift in consecutive measurements. A short is defined as a junction that has a linear ohmic *J*–*V* characteristic with a typical (contact) resistance of a few 100 Ω. An open circuit is defined as having a *J*–*V* characteristic that is independent of voltage and giving current values within the noise limit of the current meter (10^{-15} A). An unstable junction is defined as a junction not belonging to any of the other types of junctions (for example a nonsymmetric/offset junction around 0 V or a junction which displays continuously increasing current at consecutive measurements). The yield is then calculated by dividing the number of working junctions by the total number of junctions measured.

Figure 4 shows a plot of a full trace (forward and backward) log-averaged[5,23,33,41] |*J*| as a function of *V*, for different lengths of *n*-alkanethiols (n_c = 12–16). The physical explanation for taking the average of the log(|*J*|) values is that *J* depends exponentially on the thickness of the tunneling barrier, *d*, which is normally distributed.[41] Because of this, the mean, μ_{log}, and standard deviation, σ_{log}, of the log(|*J*|) data were determined. Figure S5 (Supporting Information) shows graphs of log-averaged |*J*| of the four *n*-alkanethiols separately, with ±1 standard deviation. Table S1 (Supporting Information) shows an overview of $\mu_{log} \pm \sigma_{log}$ values, determined at 1, 0.5, and 0.2 V.

A large body of work suggests nonresonant tunneling through alkanethiol SAMs.[28] For different lengths of *n*-alkanethiols, *J* roughly obeys:

$$J = J_0 e^{-\beta d} \quad (1)$$

where β (n_c^{-1}) is the decay coefficient, *d* (n_c) the thickness of the SAM and J_0 is a constant (*J* at $d = 0$) that depends on the system and includes the contact resistance.

Figure 5 shows the μ_{log} values ($\pm\sigma_{log}$) of the different *n*-alkanethiols, determined at 0.2, 0.5, and 1.0 V. The straight lines show **Equation 1** with the parameters β and J_0 (A·cm^{-2}) determined from a linear fit of ln(|*J*|). A β value of 0.72 ± 0.09 n_c^{-1} (J_0 = 1000 ± 4 A·cm^{-2}) was determined at a bias of 1 V, a β value of 0.73 ± 0.06 n_c^{-1} (J_0 = 401 ± 2 A·cm^{-2}) at 0.5 V, and a β value of 0.72 ± 0.03 n_c^{-1} (J_0 = 102 ± 2 A·cm^{-2}) at 0.2 V, showing an insignificant dependence of the β value on applied bias. A direct comparison of these data is difficult, because practically no data exist on large-area metal-molecular monolayer-metal junctions or an "interlayer" is being used to protect the SAM from shorts. When looking broader, the derived β values fall within the range of reported values in the literature (from 0.51 to 1.16), also when compared to the majority of the values (from 0.73 to 1.11).[28] It has to be noted that these data originate from many different electronic test beds, with and without an interlayer, using mono- and dithiols as the SAM and having one or two chemisorbed contacts.

When comparing the current density (3.24×10^{-3} A·cm^{-2} for C_{16} alkanethiol at 0.5 V) to other "large-area" methods, for example EGaIn (≈5×10^{-5} A·cm^{-2}),[41] or PEDOT:PSS (≈8×10^{-6} A·cm^{-2}),[5] the current density is, as expected, higher. Most likely coming from the fact that there is no protecting layer in between the SAM and metal. When comparing to the direct deposition method (≈8×10^{-1} A·cm^{-2}),[11] our method clearly has a lower current density. This is also to be expected, because it is known that direct evaporation increases defects and metal filament formation. Comparing the current density

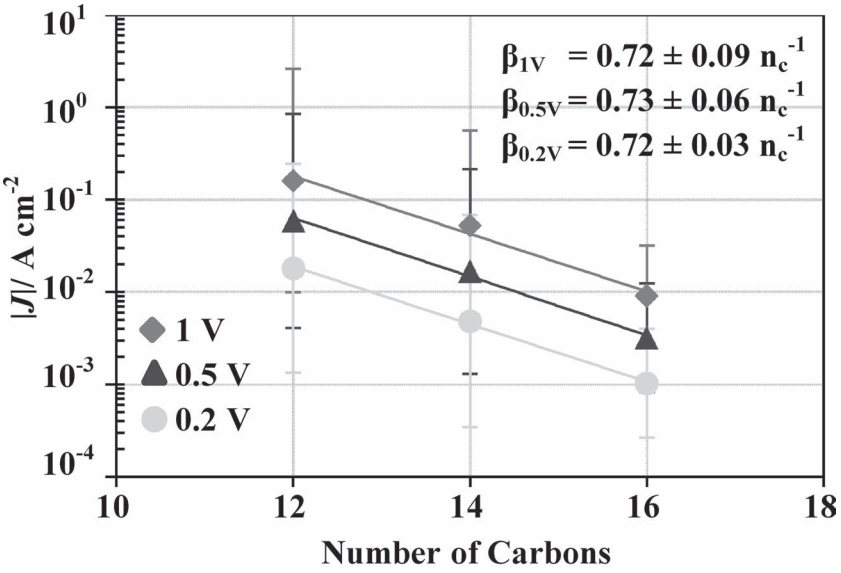

Figure 5. Plot of log-averaged |J| as a function of the number of carbon atoms, n_c, of the *n*-alkanethiol used in the junction (±1 standard deviation) at different voltages (1, 0.5, and 0.2 V), including Equation 1 (straight lines) with the parameters β and J_0 determined from a linear fit of ln(|J|).

(5.9×10^{-2} A·cm^{-2} for C_{12} alkanethiol at 0.5 V) to a fabrication method with a thin layer reduced graphene oxide as a "protective layer" ($\approx 2 \times 10^{-1}$ A·cm^{-2}),[14] where the resistance contributed by the graphene layer should be negligible, these current densities are highly comparable.

Comparing our yield (≈45%) to yields of other floatation methods (for example PALO ≈70%,[26] MoPALO, ≈80%),[27] the relatively low yield has two probable origins. The method reported here is the first case in which a floatation method is used in combination with alkanemonothiols on Au. Other floatation techniques were only shown to work in combination with Si or oxidized Al. In our case, it may be possible to improve the yield by improving the monolayer quality even more (to obtain higher contact angles and less hysteresis), but having structured bottom electrodes instead of unstructured ones, as is for example the case for (Pe)MoPALO,[27] is probably a larger problem. The structured bottom electrodes can give problems at the edges, where the SAM is less ordered, therefore more prone to metal filament formation and thus resulting in shorts. This is the most important reason why the electrodes were embedded. The structured bottom electrodes are important when considering measuring far away from the molecular junction and molecular junction integration in for example a crossbar architecture.

Even though the yield is somewhat lower, this method is an improvement from the perspective of device architecture and fabrication. Not only are thiols on Au now possible to study with floatation methods, but because this method only has a lift-off step in water, the interface between the molecular monolayer and metal top electrode is cleaner compared to the PALO/PeMoPALO method, which needs a HF detachment step and in the case of PeMoPALO has a floatation step from ethyl acetate.[30]

With the design presented here (long "thin" electrodes), we did not visually encounter any trapped water and all electrodes were well stretched without wrinkles. In case of another design (round dots embedded in the same way), however, some problems occurred with trapped water. We suggest this originates from the fact that the round dots are completely embedded in a hydrophobic area, while when using long "thin" electrodes, the water can escape to the unmodified Au sides of the molecular junctions. To further investigate that our results are not affected by trapped water in the molecular junction, a control experiment was performed by making metal-metal contacts, without a SAM in between, with the wedging transfer technique. The resulting resistances were in the range of ≈100 Ω for a 100 μm^2 junction area or lower for larger areas of the junctions. These values were in the same range as metal-metal contacts made without the floatation method, the resistance of the two leads measured separately, and as the measured shorts in the presence of a SAM in the molecular junction. Compared to the dodecanethiol SAM (average of 23.2 MΩ) this is several orders of magnitude lower. The metal-metal *I–V* curves showed clear linear behavior, indicating no problems with trapped water.

We also investigated the change of current density as a function of time and found that the small changes after several weeks, fall within the experimental error range. We tried to group the data of one thiol in different batches as a function of area and determined log-averaged current densities. These were, statistically speaking, not significantly different. Although these control experiments are convincing, we cannot completely exclude the presence of a few layers of water molecules. However, if present, such contamination has an apparently negligible effect on the charge transport.

3. Conclusions

In this study, a floatation method is presented for fabricating and electrically characterizing symmetric, large-area molecular junctions, with a relatively high yield which allows statistically relevant numbers of measurements to be obtained in a practical manner (≈500 or more complete *J*(*V*) curves on 50 or more molecular junctions per day). It is the first time that floatation methods are shown to work with metal/metal contacts, while previous reports only showed Si or oxidized Al as bottom contacts. The viability of this fabrication method was indicated by using *n*-alkanethiols as a reference system, showing an exponential length dependence of tunneling current for different lengths of *n*-alkanethiols, with a β value (0.72 ± 0.09 n_c^{-1}) ($J_0 = 1000 \pm 4$ A·cm^{-2}, determined at 1 V) which is in the range of the majority of reported values in the literature. The characteristics of the fabrication method now permits straightforward extension of this system to a variety of molecules and electrodes,

and the study of the relationship between organic structure and tunneling current in monolayers, without the problem of introducing ambiguities in the interpretation of data.

When using no additional, protecting layer on top of the monolayer, it appeared crucial to apply the top electrodes as gently as possible. Manual application of ultra-smooth top electrodes embedded in OA on a PDMS stamp worked, but the approach was probably not gentle enough, as indicated by a yield of ≈10%. Applying the top electrodes with the wedging transfer method is a softer procedure and resulted in a greatly enhanced yield.

As both the bottom and top electrodes are ultra-smooth and structured by photolithography, this method can be extended to other metals, as long as the metal is poorly adhering to the native SiO_2. This gives the opportunity to study the influence of the metal work function on the electronic performance of molecular monolayer devices. Equally important is that combination of the photolithographic electrode patterning with an alignment step while applying the top electrode opens the door to integration into more complex devices.

4. Experimental Section

General Information: Single side polished p-type Si(100) wafers were purchased from Okmetic. Cellulose acetate butyrate (average $M_n \approx 30$ kDa) and 1-dodecanethiol (≥98%) were purchased from Sigma Aldrich. 1-Tetradecanethiol (≥98%) and 1-hexadecanethiol (≥95%) were purchased from Fluka. 1H,1H,2H,2H-Perfluorodecyltrichlorosilane (PFDTS, ≥97%) was purchased from ABCR GmbH. Negative photoresist (TI 35 ES) was purchased from MicroChemicals and developer, Olin OPD 6242, was purchased from FujiFilm. HMDS was purchased from BASF. Optical adhesive (No. 61) was purchased from Norland. Solvents were of analytical grade, except for ethyl acetate (technical grade). All chemicals were used as received.

Electrode Fabrication: The following procedure was used for fabricating Au electrodes without an adhesion layer. The negative photoresist TI 35ES was used as a metal lift-off mask to generate the electrode pattern. This resist was chosen for the negatively tapered sidewalls, which is preferred in single-layer lift-off. First, the electrode pattern was created in the negative resist. The process started with spincoating an adhesion layer, HMDS (5 s 500 rpm, 30 s 4000 rpm), after which TI 35ES was spincoated (5 s 500 rpm, 30 s 4000 rpm) followed by a pre-exposure bake step (2 min, 95 °C). The photoresist was exposed (20 s, EVG EV620 Mask Aligner, Hg-lamp 12 mW·cm^{-2}) through a patterned photomask, followed by a degassing step (30 min), a post-exposure bake (2 min, 120 °C) and a flood exposure (60 s, no mask). The wafer was then developed in Olin OPD 4262 (60 s) and rinsed with Milli-Q water in a quickdump rinser. Prior to metal evaporation, the wafer was cleaned with UV-ozone (PR-100, UVP inc) for 30 min, guaranteeing a clean and poorly adhering native silicon oxide substrate. Immediately after this step, 100 nm Au was evaporated (BAK 600, Balzers), with a deposition rate between 2–4 Å s^{-1} ($<10^{-6}$ mbar). This evaporation needs to be controlled carefully: a too low evaporation rate resulted in damaged electrodes at the metal lift-off step while a too high evaporation rate resulted in incomplete template stripping. After the evaporation step, metal lift-off was performed by placing the wafer gently in a resist stripper (Baker PRS 2000) for 60 min. When the lift-off was tried in acetone, the wafer did not completely clean. Normally, a sonication step is also used, but this destroys the Au electrodes when no adhesion layer is used. Afterwards the wafer was gently dipped in a beaker with deionized water, followed by spin-drying.

The bottom electrodes were prepared for template stripping (TS). To lower the adhesion of OA to the Si/SiO_2 first an anti-sticking layer of PFDTS was deposited from the gas phase for 60 min by adding 0.05 mL PFDTS with the substrate in a dessicator, which was pumped down for 10 min.[6] Then drops of OA were applied on top of the bottom electrodes. After applying freshly cleaned glass slides (Thermo Scientific microscopic slides, 1 mm thick, cleaned with piranha for 30 min) on top of the drops, the OA was UV-cured for 2 h. This resulted in a sandwich of Si/SiO_2/Au/OA/glass where the interface between SiO_2 and Au was the weakest.

The Au/OA/glass composite was template stripped from the wafer by applying a razor blade at a low angle, with respect to the wafer, at a corner of the glass slide. When applying a small force parallel to the wafer, the Au/OA/glass composite separated from the wafer, which exposed the ultra-flat Au electrodes embedded in the OA.

SAM Preparation: All *n*-alkanethiol SAMs were prepared by the same method. After TS of the bottom electrodes, the substrate was immersed in an ethanolic solution of the thiol of choice (5 mM) as soon as possible. The solution was kept overnight (≈18 h) under an argon atmosphere. After SAM formation, the substrate was gently rinsed with ethanol and dried with N_2. The quality of the SAMs was checked by contact angle measurements. Table S2 (Supporting Information) shows the static and dynamic water contact angles and the contact angle hysteresis for all alkanethiol SAMs.

Wedging Transfer: The wedging transfer technique was adopted from ref. [32]. In short, the substrate with top electrodes on it was dipped for 5 s into a cellulose acetate butyrate solution (30 mg/mL in ethyl acetate), including 1-dodecanethiol (0.1 vol%) to enhance the sticking of the polymer to the Au. The polymer was dried under ambient conditions for 3 min. In order to allow good wedging transfer, the polymer was dissolved at the bottom and edges of the substrate with a cotton swab dipped in ethyl acetate. The wafer was then slowly dipped into Milli-Q water under an angle of ≈70°, separating the hydrophobic polymer from the hydrophilic wafer. This resulted in a floating polymer layer with the Au electrodes embedded, with the ultra-smooth interface facing downwards. The top electrodes embedded in the cellulose acetate butyrate were manipulated with a micromanipulator while the water level was slowly decreased by a syringe pump. Alignment was done by eye, but when done under a microscope the accuracy would be on the order of microns. With a better micromanipulator a sub-micrometer accuracy can be obtained.[32] After contact was made, the molecular junction device was placed in a desiccator and pumped down overnight to evaporate possible remaining water between the top and bottom contacts. The setup used is shown in Figure S6 in the Supporting Information.

Electrical Measurements: The electrical measurements were done with a Karl Süss probe station connected to a Keithley 4200 semiconductor characterization system. The current-voltage curves were measured by varying the applied voltage in steps of 5 mV from 0 V → 1 V → –1 V → 0 V. Each full trace thus gave two current data points at each voltage value, one from the forward and one from the backward sweep. For all calculations and fitting (except for Figure 4) the forward and backward $J(V)$ trace were used together. The applied voltage was started at 0 V to avoid rapid voltage changes across the molecular junction which would otherwise result in turn-on phenomena. The J–V curves were not reproducible when the applied voltage started directly at 1 V. When a non-short junction was measured, the measurement would be repeated another ten times.

AFM Measurements: The surface topography of freshly template-stripped Au bottom electrodes was analyzed by atomic force microscopy (AFM) under ambient conditions with a Veeco (Bruker) Dimension 3100. Images across various scan areas were recorded in tapping mode using a rectangular silicon cantilever (nanosensors PPP-NCHR) with a tip diameter of ≈7 nm and a spring constant of 42 N/m. The rms roughness of the electrodes was determined by averaging over 30 areas from three different electrodes, where each area was 2 μm × 2 μm.

Supporting Information

Supporting Information is available from the Wiley Online Library or from the author.

Acknowledgements

The authors thank Maaike Heitink for designing the pictures of Figure 1. This work was supported by the Council for Chemical Sciences of the Netherlands Organization for Scientific Research (NWO-CW, Vici grant 700.58.443 to J.H.). W.G.v.d.W. acknowledges financial support from the European Research Council, ERC Starting Grant no. 240433 and from the NWO-nano program, grant no.11470.

Received: March 2, 2012
Revised: August 22, 2012
Published online: September 24, 2012

[1] R. L. McCreery, A. J. Bergren, *Adv. Mater.* **2009**, *21*, 4303.
[2] C. P. Collier, E. W. Wong, M. Belohradský, F. M. Raymo, J. F. Stoddart, P. J. Kuekes, R. S. Williams, J. R. Heath, *Science* **1999**, *285*, 391.
[3] J. E. Green, J. Wook Choi, A. Boukai, Y. Bunimovich, E. Johnston-Halperin, E. DeIonno, Y. Luo, B. A. Sheriff, K. Xu, Y. Shik Shin, H.-R. Tseng, J. F. Stoddart, J. R. Heath, *Nature* **2007**, *445*, 414.
[4] H. B. Akkerman, P. W. M. Blom, D. M. de Leeuw, B. de Boer, *Nature* **2006**, *441*, 69.
[5] P. A. Van Hal, E. C. P. Smits, T. C. T. Geuns, H. B. Akkerman, B. C. De Brito, S. Perissinotto, G. Lanzani, A. J. Kronemeijer, V. Geskin, J. Cornil, P. W. M. Blom, B. De Boer, D. M. De Leeuw, *Nat. Nanotechnol.* **2008**, *3*, 749.
[6] C. A. Nijhuis, W. F. Reus, J. R. Barber, M. D. Dickey, G. M. Whitesides, *Nano Lett.* **2010**, *9*, 3611.
[7] A. S. Blum, J. G. Kushmerick, D. P. Long, C. H. Patterson, J. C. Yang, J. C. Henderson, Y. Yao, J. M. Tour, R. Shashidhar, B. R. Ratna, *Nat. Mater.* **2005**, *4*, 167.
[8] R. L. McCreery, *ChemPhysChem* **2009**, *10*, 2387.
[9] M. Halik, A. Hirsch, *Adv. Mater.* **2011**, *23*, 2689.
[10] J. C. Love, L. A. Estroff, J. K. Kriebel, R. G. Nuzzo, G. M. Whitesides, *Chem. Rev.* **2005**, *105*, 1103.
[11] T. Kim, G. Wang, H. Lee, T. Lee, *Nanotechnology* **2007**, *18*, 315204.
[12] R. Haag, M. A. Rampi, R. E. Holmlin, G. M. Whitesides, *J. Am. Chem. Soc.* **1999**, *121*, 7895.
[13] G. Wang, Y. Kim, M. Choe, T.-W. Kim, T. Lee, *Adv. Mater.* **2011**, *23*, 755.
[14] S. Seo, M. Min, J. Lee, T. Lee, S.-Y. Choi, H. Lee, *Angew. Chem. Int. Ed.* **2012**, *51*, 108.
[15] R. C. Chiechi, E. A. Weiss, M. D. Dickey, G. M. Whitesides, *Angew. Chem. Int. Ed.* **2008**, *47*, 142.
[16] C. A. Nijhuis, W. F. Reus, G. M. Whitesides, *J. Am. Chem. Soc.* **2009**, *131*, 17814.
[17] Y.-L. Loo, D. V. Lang, J. A. Rogers, J. W. P. Hsu, *Nano Lett.* **2003**, *3*, 913.
[18] M. A. Reed, C. Zhou, C. J. Muller, T. P. Burgin, J. M. Tour, *Science* **1997**, *278*, 252.
[19] M. Coll, L. H. Miller, L. J. Richter, D. R. Hines, O. D. Jurchescu, N. Gergel-Hackett, C. A. Richter, C. A. Hacker, *J. Am. Chem. Soc.* **2009**, *131*, 12451.
[20] B. Xu, N. J. Tao, *Science* **2003**, *301*, 1221.
[21] D. J. Wold, C. D. Frisbie, *J. Am. Chem. Soc.* **2000**, *122*, 2970.
[22] V. B. Engelkes, J. M. Beebe, C. D. Frisbie, *J. Am. Chem. Soc.* **2004**, *126*, 14287.
[23] V. B. Engelkes, J. M. Beebe, C. D. Frisbie, *J. Phys. Chem. B* **2005**, *109*, 16801.
[24] G. Wang, T.-W. Kim, G. Jo, T. Lee, *J. Am. Chem. Soc.* **2009**, *131*, 5980.
[25] A. Vilan, D. Cahen, *Adv. Funct. Mater.* **2002**, *12*, 795.
[26] K. T. Shimizu, J.D. Fabbri, J. J. Jelincic, N. A. Melosh, *Adv. Mater.* **2006**, *18*, 1499.
[27] N. Stein, R. Korobko, O. Yaffe, R. Har Lavan, H. Shpaisman, E. Tirosh, A. Vilan, D. Cahen, *J. Phys. Chem. C* **2010**, *114*, 12769.
[28] H. B. Akkerman, B. de Boer, *J. Phys.: Condens. Matter* **2008**, *20*, 20.
[29] A. Salomon, T. Böcking, J. J. Gooding, D. Cahen, *Nano Lett.* **2006**, *6*, 2873.
[30] Because of the increased rigidity of the layer in PeMoPALO, a different solvent system was used. A two-phase system, 1:4 (v/v) water-methanol and ethyl acetate, was necessary, where the metal electrodes and polymer layer floats at the liquid/liquid interface. Using ethyl acetate affected the electrical measurements. This points to a different interface between the monolayer and top electrode, which was not the case when water was used (see the Supporting Information of ref. [27]).
[31] E. A. Weiss, G. K. Kaufman, J. K. Kriebel, Z. Li, R. Schalek, G. M. Whitesides, *Langmuir* **2007**, *23*, 9686.
[32] G. g. F. Schneider, V. E. Calado, H. Zandbergen, L. M. K. Vandersypen, C. Dekker, *Nano Lett.* **2010**, *10*, 1912.
[33] E. A. Weiss, R. C. Chiechi, G. K. Kaufman, J. K. Kriebel, Z. Li, M. Duati, M. A. Rampi, G. M. Whitesides, *J. Am. Chem. Soc.* **2007**, *129*, 4336.
[34] D. Stamou, D. Gourdon, M. Liley, N. A. Burnham, A. Kulik, H. Vogel, C. Duschl, *Langmuir* **1997**, *13*, 2425.
[35] A. J. Black, K. E. Paul, J. Aizenberg, G. M. Whitesides, *J. Am. Chem. Soc.* **1999**, *121*, 8356.
[36] K. A. Dill, T. M. Truskett, V. Vlachy, B. Hribar-Lee, *Annu. Rev. Biophys. Biomol. Struct.* **2005**, *34*, 173.
[37] N. T. Southall, K. A. Dill, A. D. J. Haymet, *J. Phys. Chem. B* **2001**, *106*, 521.
[38] M. Ø. Jensen, O. G. Mouritsen, G. H. Peters, *J. Chem. Phys.* **2004**, *120*, 9729.
[39] J. Janeček, R. R. Netz, *Langmuir* **2007**, *23*, 8417.
[40] C. Sendner, D. Horinek, L. Bocquet, R. R. Netz, *Langmuir* **2009**, *25*, 10768.
[41] M. M. Thuo, W. F. Reus, C. A. Nijhuis, J. R. Barber, C. Kim, M. D. Schulz, G. M. Whitesides, *J. Am. Chem. Soc.* **2011**, *133*, 2962.